Analysis of ultrathin SiO_2 interface layers in chemical vapor deposition of Al_2O_3 on Si by *in situ* scanning transmission electron microscopy

R. F. Klie[a)]
Materials Science Department, Brookhaven National Laboratory, Upton, New York 11973

N. D. Browning
Department of Chemical Engineering and Materials Science, University of California-Davis, Davis, California 95616

A. Roy Chowdhuri and C. G. Takoudis
Department of Chemical Engineering, University of Illinois at Chicago, Chicago, Illinois 60607-7000

(Received 18 September 2002; accepted 31 May 2003)

The development of Al_2O_3 as an alternative gate dielectric for microelectronic applications depends on the ability to grow a high-quality nanoscale thin film that forms an atomically abrupt interface with Si. Here, the combination of *in situ* Z-contrast imaging, electron energy loss spectroscopy and x-ray photoelectron spectroscopy of amorphous Al_2O_3 films grown by metalorganic chemical vapor deposition shows that excess oxygen incorporated into the film routinely reacts with the Si substrate to form an amorphous SiO_2 interface layer during postdeposition annealing. The intrinsic oxygen-rich environment of all films grown by such techniques and the necessity of postdeposition processing in device applications implies that control and optimization of the SiO_2 interface layers could be of utmost interest for high-κ dielectric stacked structures. © *2003 American Institute of Physics.* [DOI: 10.1063/1.1597415]

One of the key challenges facing the continued advancement of integrated circuit technology over the next five years is the identification of high-κ dielectric materials. Aluminum oxide (Al_2O_3) has gathered considerable interest, primarily due to its potential to replace SiO_2 as the dielectric layer in complementary metal–oxide–semiconductor device fabrication.[1] Besides having a dielectric constant which is more than twice that of SiO_2, Al_2O_3 has a band gap of ~ 9 eV with 2.8 eV conduction band offset to Si. Furthermore, perhaps the most notable of the desirable properties is the ability of *stoichiometric* Al_2O_3 to form a thermodynamically stable interface[1,2] with Si. This is in fact a considerable advantage, as in order to function as a high-κ material and deliver low electrical thickness (or higher gate capacitance) with a larger physical thickness, the formation of a low-κ SiO_2 interface layer must be prevented. However, the O/Al ratio of ultrathin (<10 nm) aluminum oxide films, obtained by processes that are currently employed for deposition depends sensitively on the process, and may be considerably higher than stoichiometric Al_2O_3.[3–7] In such cases, the interface with Si may not be as stable and this issue assumes key importance in determining the applicability of Al_2O_3 to next generation integrated circuits.

In this letter we present direct atomic scale analyses of the interface between *nonstoichiometric* metalorganic chemical vapor deposited ultrathin aluminum oxide films and Si (100) during *in situ* annealing. It is important to note here that the nonstoichiometry is a natural result of the growth process in trimethyl aluminum (TMA) and O_2 and not an artifact deliberately introduced into the experiment. The deposition of the films was carried out under standard conditions of 300 °C and 0.5 Torr using TMA (Akzo Nobel) and oxygen in a custom-built low-pressure chemical vapor deposition chamber.[8] (For more details see Ref. 9). Prior to the deposition, the substrate [double polished *n*-Si(100) float zone wafer] was thoroughly cleaned to remove organic contamination and native oxide from the surface. The expected native oxide growth-rate on such a substrate is less than 0.5 nm in 30 min under continuous exposure to O_2 at 300 °C.

The films were characterized by a combination of atomic-resolution *Z*-contrast imaging, electron energy-loss spectroscopy (EELS) in the scanning transmission electron microscope (STEM), x-ray photoelectron spectroscopy (XPS), and Fourier-transform infrared (FTIR) spectroscopy. These techniques were used to investigate the structural and chemical changes that occur in the films during the postdeposition annealing step. The combination of *Z*-contrast imaging (which can identify small changes in atomic number) and electron energy loss spectroscopy (which can quantify composition and bonding fluctuations) can provide an accurate description of the structure and chemistry of the interface with high spatial resolution (<2 Å). *Z*-contrast images and EELS spectra were also obtained while the as-deposited sample was heated *in situ* inside the STEM. As the partial pressure of O_2 inside the microscope column is $\sim 5 \times 10^{-8}$ Pa, any observed changes in the interface structure originate from the diffusion of oxygen present in the original sample.

The STEM and EELS results presented in this letter were obtained using a JEOL 2010F STEM/TEM, having a Schottky field emission gun-source and being operated at 200 kV.[10,11] The microscope is equipped with a standard ''ultra high resolution'' objective lens pole piece, a JEOL annular dark-field detector and a postcolumn Gatan imaging filter.[9,10] The experimental setup for this microscope ($a = 13$ mrad, $\theta_c = 52$ mrad) allows us to use low-angle scattered electrons that do not contribute to the incoherent *Z*-contrast image for EELS.[12] As the two techniques do not

a)Electronic mail: klie@bnl.gov

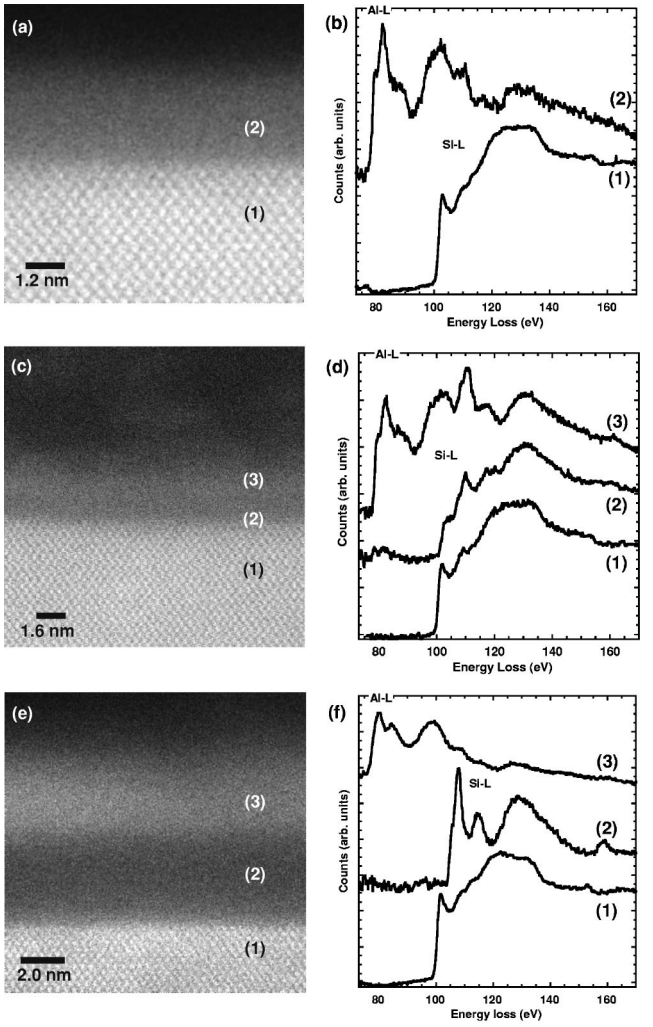

FIG. 1. *Z*-contrast image of the film (a) *as deposited*, (c) after *in situ* heating inside the microscope for 79 min at 500 °C, and (e) *ex situ* annealing in Ar for 25 min at 900 °C. The corresponding background subtracted and multiple scattering corrected EELS spectra ($\Delta E = 1.0$ eV) are shown in (b), (d), and (f).

interfere, *Z*-contrast images can be used to position the electron probe at the desired spot in the sample to acquire spectra.[13–15] Several spectra with acquisition times of ~ 0.5 s are acquired consecutively in each position and compared to ensure that the beam damage is not contributing significantly to the observed spectral changes. For the *in situ* heating experiments, a Gatan double tilt heating holder was used, with a variable temperature range up to 1000 °C. The temperature is measured at the heating coils of the specimen holder and does not necessarily represent the actual specimen temperature. Hence, for short heating cycles and samples with poor thermal conductivity, the sample temperature might be significantly lower than indicated. The specimen drift obtained with this holder is less than 1 nm per minute for temperatures below 500 °C.[16]

Figure 1(a) shows an atomic resolution *Z*-contrast image of the amorphous $Al_2O_{3+\delta}$ film on the clean Si (100) substrate. The film thickness is determined to be (3.5 ± 0.2) nm and the Si substrate is located at the bottom of the micrograph. The interface between the substrate and the film appears atomically abrupt. Figure 1(b) displays EEL spectra taken from locations indicated in Fig. 1(a). The spectrum from the Si substrate contains the Si–L edges with an edge-onset at (99.8 ± 0.5) eV due to Si^0 contribution but no distinct white line intensities that would indicate a native oxide.[17] The *as-deposited* film spectrum contains a strong Al–L edge (onset: 78.2 ± 0.5 eV), characteristic of amorphous Al_2O_3 and no measurable intensities at either the Si^0 or the Si^{4+} core-loss onsets.

Figure 1(c) shows the same specimen region after several *in situ* heating cycles to nominally 500 °C that amount to a total heating time of 79 min. The interface between the substrate and the film appears darker now and the overall film thickness is increased to (4.3 ± 0.2) nm. The EEL-spectra [Fig. 1(d)] show an unaltered Si–L edge fine structure in the Si support (spectrum 1), but the Si–L edge of the darker region at the substrate-film interface (spectrum 2) exhibits characteristic features of both Si^0 and Si^{4+}, indicated by the unaltered edge onset and the distinct L_3, L_2 white lines at (110 ± 0.5) eV and (117.6 ± 0.5) eV, respectively. This can be interpreted as being caused by a change from predominantly Si^0 to mixed Si^0–Si^{4+} contributions in the spectrum. Spectrum 3, taken from the deposited film shows the Al–L edge [onset: (78.0 ± 0.5) eV] and contribution from Si^{4+}, indicating that the interface between the amorphous Al_2O_3 film and the Si substrate contains a significant amount of SiO_2 that was formed during the *in situ* heating process *inside* the STEM. It is important to note again, that the partial pressure of oxygen inside the microscope is so low that any change in the interface structure must originate from oxygen trapped in the *as-deposited* film.

Figure 1(e) shows a high-resolution *Z*-contrast image of a 5 nm film annealed for 25 min in Ar at 900 °C. The dark region (5 nm) in between the Si and the brighter Al_2O_3 film indicates a-SiO_2. The silicon–oxide layer EEL spectrum [Fig. 1(f)] shows a shift of the edge onset with respect to the Si substrate spectrum of (6.2 ± 0.5) eV and a distinct L_3, L_2 splitting. No aluminum signal is detected, thus indicating a pure SiO_2 layer. The aluminum oxide film spectrum contains a strong Al peak[18,19] (onset: 77.2 ± 0.5 eV) characteristic of amorphous Al_2O_3 and no measurable intensities at either the Si^0 or the Si^{4+} core-loss onsets.

The XPS and FTIR analysis of the samples, both before and after annealing corroborates the observations made in the *in situ* STEM study. The results of the FTIR study were previously reported[9] and showed the thermal growth of an a-SiO_2 layer upon *ex situ* high-temperature annealing. The XPS (Kratos, AXIS Ultra XPS) spectrum (Fig. 2) shows the Si $2p$ signal obtained from a 6 nm *as-deposited* film (spectrum a). The Si $2p$ peak appearing at 99.3 eV is from Si^0. The absence of any signal from Si^{n+} $(n>0)$ provides another confirmation of the absence of SiO_2 in the *as-deposited* samples. The Al $2p$ signal for the *as-deposited* films (not shown here) at 75.4 eV indicates the presence of only the Al^{3+} state.[3,20,21] The *as-deposited* film was annealed at 500 °C (spectrum b) and 900 °C (spectrum c) in Ar for 10 min in a quartz furnace. In both cases the Si $2p$ signal shows distinct peaks from the Si^0 (99.3 eV) and Si^{+4} (102.9 eV) states. The Si^{4+} intensity relative to the Si^0 is larger for the sample annealed at 900 °C suggesting that the thickness of SiO_2 layer formed during annealing is larger for higher annealing temperatures. The Al $2p$ signal in the annealed

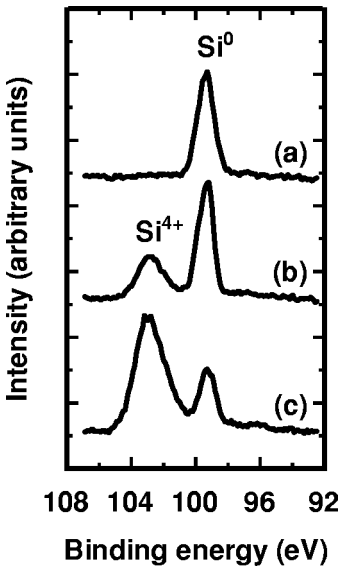

FIG. 2. XPS spectra of the Si 2*p* signal in films deposited at 300°C. (a) As-deposited, film (b) after 10 min annealing in Ar at 500 °C, and (c) 900 °C.

samples shifts slightly to higher binding energies indicating a change in the chemical environment of the Al_2O_3 film as a result of annealing.

The O/Al and O/Si^{4+} ratio for the samples were calculated from integrated peak intensities and the atomic sensitivity factor of each species. For the annealed samples, the O 1*s* peak was deconvoluted into two components each corresponding to the oxygen associated with Al^{3+} and Si^{4+} states. In the *as-deposited* samples the O/Al ratio was (2.1 ± 0.1). Annealing at 500 °C was found to decrease this ratio to 1.7 ± 0.1, while annealing at 900 °C reduced it to (1.5 ± 0.1), close to the O/Al ratio in stoichiometric Al_2O_3. In both cases the O/Si^{4+} ratio was close to that of stoichiometric SiO_2. With the equipment used in this study, the practical detection-limit of the XPS measurements was ~ 1 monolayer. This limit may increase with to the presence of Al_2O_3, nevertheless, the absence of SiO_2 at the interface has also been confirmed by FTIR, which can detect sub monolayer films of SiO_2.[20]

This study shows that ultra-thin *as-deposited* amorphous aluminum oxide films can form an atomically abrupt interface with Si. However, the chemical vapor deposition method with TMA and O_2 results in the aluminum oxide film being oxygen rich. This nonstoichiometry leads to a thermodynamically different condition than is present in stoichiometric films and the interface stability suffers as a result of it. We provide direct evidence for three different annealing conditions, which all show the formation of an interstitial silicon oxide layer upon high temperature treatment at low oxygen partial pressure. Hence, the formation of the a-SiO_2 layer at the film-substrate interface during annealing can only be explained by considering diffusion of the excess oxygen present in the film towards the substrate and reacting to form SiO_2. The increase in film thickness upon *in situ* heating and the change in the Al–L edge onset (from 78.0 to 77.2 eV) support this hypothesis. This oxidation process continues until the equilibrium thickness is attained and the aluminum oxide film becomes stoichiometric. The *ex situ* annealed samples represent this equilibrium state. The results from the atomic resolution STEM study of *in situ* annealed Al_2O_3/Si indicate that there may be intriguing design issues in the use of amorphous Al_2O_3 as a high-κ dielectric in integrated circuit technology and that increased applicability can be obtained by developing methods to control and optimize the excess oxygen in the *as-deposited* films.

Experimental results were obtained on the JEOL 2010F, operated by the Research Resources Center at UIC and funded by NSF under Grant No. DMR-9601796. This research was supported in part by NSF under Grant No. DMR-9733895 and CTS 9813984. The XPS data were obtained at the Center for Microanalysis of Materials, UIUC supported by the U.S. Department of Energy under Grant No. DEFG02-96-ER45439.

[1] G. D. Wilk, R. M. Wallace, and J. M. Anthony, J. Appl. Phys. **89**, 5243 (2001).
[2] S. Guha, E. Cartier, N. A. Bojarczuk, J. Bruley, L. Gignac, and J. Karasinski, J. Appl. Phys. **90**, 512 (2001).
[3] Y.-C. Kim, H.-H. Park, J. S. Chun, and W.-J. Lee, Thin Solid Films **237**, 57 (1994).
[4] Z. Katz-Tsameret and A. Raveh, J. Vac. Sci. Technol. A **13**, 1121 (1995).
[5] B. G. Segda, M. Jacquet, and J. P. Besse, Vacuum **62**, 27 (2001).
[6] E. P. Gusev, M. Copel, and E. Cartier, Appl. Phys. Lett. **76**, 176 (2000).
[7] T. M. Klein, D. Niu, W. S. Epling, W. Li, D. M. Maher, C. C. Hobbs, R. I. Hegde, I. J. R. Baumvol, and G. N. Parsons, Appl. Phys. Lett. **75**, 4001 (1999).
[8] Z. Cui, J. Madsen, and C. G. Takoudis, J. Appl. Phys. **87**, 8181 (2000).
[9] A. Roy Chowdhuri, C. G. Takoudis, R. F. Klie, and N. D. Browning, Appl. Phys. Lett. **80**, 4241 (2002)
[10] E. M. James and N. D. Browning, Ultramicroscopy **78**, 125 (1999).
[11] E. M. James, N. D. Browning, A. W. Nicholls, M. Kawasaki, Y. Xin, and S. Stemmer, J. Electron Microsc. **47**, 561 (1998).
[12] R. F. Egerton, *Electron Energy Loss Spectroscopy in the Electron Microscope* (Plenum, New York, 1986).
[13] N. D. Browning, M. F. Chrisholm, and S. J. Pennycook, Nature (London) **366**, 143 (1993).
[14] P. D. Nellist and S. J. Pennycook, Ultramicroscopy **78**, 111 (1999).
[15] D. E. Jesson and S. J. Pennycook, Proc. R. Soc. London, Ser. A **449**, 273 (1995).
[16] R. F. Klie and N. D. Browning, Appl. Phys. Lett. **77**, 3737 (2000).
[17] P. E. Batson, Nature (London) **366**, 727 (1993)
[18] K. Suenaga, D. Bouchet, C. Colliex, A. Thorel, and D. G. Brandon, J. Eur. Ceram. Soc. **18**, 1453 (1998).
[19] M. Halvarsson, A. Larsson, and S. Ruppi, Micron **32**, 807 (2001).
[20] Q. Wang, W. Zhao, J. Lozano, Y.-M. Sun, C. G. Willson, and J. M. White, Appl. Surf. Sci. **183**, 182 (2001).
[21] E. Paparazzo, Vacuum **62**, 47 (2001).